Optical properties of wurtzite and zinc-blende GaN/AlN quantum dots

Vladimir A. Fonoberov[a] and Alexander A. Balandin[b]
Nano-Device Laboratory, Department of Electrical Engineering, University of California—Riverside, Riverside, California 92521

(Received 19 January 2004; accepted 23 March 2004; published 20 August 2004)

We investigate theoretically and compare optical properties of wurtzite and zinc-blende GaN/AlN quantum dots with heights from 1.5 to 4.5 nm. The quantum dot size corresponds to the strong quantum confinement regime. It has been established that the built-in piezoelectric field at the GaN/AlN interface governs optical properties of wurtzite quantum dots while having a small effect on zinc-blende quantum dots. The strain field strongly modifies the excitonic states in both wurtzite and zinc-blende GaN/AlN quantum dots. It has been shown that the radiative lifetime dependence on the quantum dot height is very different in the zinc-blende and wurtzite quantum dots. The excitonic optical properties of GaN/AlN quantum dots calculated using our model are in good agreement with available experimental data. Reported theoretical results for the optical spectra of GaN/AlN quantum dots can be used for interpretation of experimental data and optimization of the quantum dot structures for optoelectronic applications.
[DOI: 10.1116/1.1768188]

I. INTRODUCTION

Reports of fabrication of GaN/AlN quantum dots (QDs)[1–3] have attracted significant attention due to the fact that GaN-based nanostructures are considered to be promising candidates for electronic, optical, and optoelectronic applications. Further progress in GaN technology has led to an increasing number of publications on fabrication[2–4] and characterization[5,6] of wurtzite (WZ) as well as zinc-blende (ZB) GaN/AlN QDs. Despite the large number of reports on fabrication and experimental optical characterization of WZ and ZB GaN/AlN QDs, there have been a small number of theoretical studies of optical properties of GaN/AlN QDs.[7,8] The lack of accurate theoretical models and calculations makes it difficult to interpret experimental data and find the optimum QD structure parameters for the proposed applications. A particularly important problem, which has not been addressed in sufficient detail, is the physics of GaN/AlN interface and the role of the strain fields and piezoelectric built-in field at the interface in the optical response of GaN/AlN QDs.

In this article, we theoretically investigate the dependence of the excitonic optical properties of WZ and ZB GaN/AlN QDs, focusing on their QD size dependence. The similarities and distinctions between the two types of GaN/AlN QDs with different crystal structures and geometries are discussed. The obtained theoretical results are then compared with available experimental data.

II. THEORETICAL MODEL

In order to calculate exciton states in WZ and ZB GaN/AlN QDs we use the theoretical model and calculation procedures described in Ref. 7. The model allows us to take into account the strain and piezoelectric fields at the interface between GaN QD and AlN barrier materials. It also explicitly includes degeneracy and anisotropy of conduction and valence bands. In this section, we briefly describe the theoretical model extended to calculate exciton states, oscillator strengths, and radiative lifetimes in GaN/AlN QDs.

Since the strain tensor $\varepsilon_{ij}(\mathbf{r})$ is symmetric, it can be presented in the following form:

$$\varepsilon_{ij}=\begin{pmatrix}\varepsilon_1 & \varepsilon_6 & \varepsilon_5\\ \varepsilon_6 & \varepsilon_2 & \varepsilon_4\\ \varepsilon_5 & \varepsilon_4 & \varepsilon_3\end{pmatrix}. \tag{1}$$

The six components of the strain tensor (1) are not independent and can be expressed through the three components of the displacement vector $\mathbf{u}(\mathbf{r})$ as follows:

$$\varepsilon_1=\frac{\partial u_x}{\partial x}-\frac{a(\mathbf{r})-a_0}{a_0};\quad \varepsilon_4=\frac{1}{2}\left(\frac{\partial u_y}{\partial z}+\frac{\partial u_z}{\partial y}\right);$$
$$\varepsilon_2=\frac{\partial u_y}{\partial y}-\frac{a(\mathbf{r})-a_0}{a_0};\quad \varepsilon_5=\frac{1}{2}\left(\frac{\partial u_x}{\partial z}+\frac{\partial u_z}{\partial x}\right); \tag{2}$$
$$\varepsilon_3=\frac{\partial u_z}{\partial z}-\frac{c(\mathbf{r})-c_0}{c_0};\quad \varepsilon_6=\frac{1}{2}\left(\frac{\partial u_x}{\partial y}+\frac{\partial u_y}{\partial x}\right).$$

In Eq. (2), $a(\mathbf{r})$ and $c(\mathbf{r})$ are the lattice constants of GaN when $\mathbf{r}$ is inside the QD and the lattice constants of AlN (denoted as a_0 and c_0) when $\mathbf{r}$ is outside the QD. Note that $c(\mathbf{r})=a(\mathbf{r})$ and $c_0=a_0$ for ZB GaN/AlN QDs.

The strain tensor (1) is found by minimizing the elastic energy

$$F_{\text{elastic}}=\frac{1}{2}\int_V d\mathbf{r}\sum_{k,n=1}^{6} C_{kn}(\mathbf{r})\varepsilon_k(\mathbf{r})\varepsilon_n(\mathbf{r}) \tag{3}$$

with respect to $\mathbf{u}(\mathbf{r})$. In Eq. (3) V is the volume of the system and $C_{kn}(\mathbf{r})$ is the tensor of elastic moduli of GaN when $\mathbf{r}$ is

[a]Electronic mail: vladimir@ee.ucr.edu
[b]Electronic mail: alexb@ee.ucr.edu

TABLE I. Lattice, elastic, piezoelectric, and dielectric parameters from Ref. 7.

Parameters	WZ GaN	WZ AlN	Parameters	ZB GaN	ZB AlN
a (nm)	3.189	3.112	a (nm)	4.50	4.38
c (nm)	5.185	4.982			
C_{11} (GPa)	390	396	C_{11} (GPa)	293	304
C_{12} (GPa)	145	137	C_{12} (GPa)	159	160
C_{13} (GPa)	106	108	C_{44} (GPa)	155	193
C_{33} (GPa)	398	373			
C_{44} (GPa)	105	116			
e_{15} (C/m^2)	−0.49	−0.60	e_{14} (C/m^2)	0.50	0.59
e_{31} (C/m^2)	−0.49	−0.60			
e_{33} (C/m^2)	0.73	1.46			
P_{sp} (C/m^2)	−0.029	−0.081			
$\varepsilon_{stat}^{\parallel}$	10.01	8.57	ε_{stat}	9.7	9.7
$\varepsilon_{stat}^{\perp}$	9.28	8.67			

inside the QD and the tensor of elastic moduli of AlN when $\mathbf{r}$ is outside the QD. For WZ and ZB GaN/AlN QDs, the tensors of elastic moduli are given as

$$C_{kn}^{WZ}=\begin{pmatrix} C_{11} & C_{12} & C_{13} & 0 & 0 & 0 \\ C_{12} & C_{11} & C_{13} & 0 & 0 & 0 \\ C_{13} & C_{13} & C_{33} & 0 & 0 & 0 \\ 0 & 0 & 0 & 4C_{44} & 0 & 0 \\ 0 & 0 & 0 & 0 & 4C_{44} & 0 \\ 0 & 0 & 0 & 0 & 0 & 2(C_{11}-C_{12}) \end{pmatrix};$$

$$C_{kn}^{ZB}=\begin{pmatrix} C_{11} & C_{12} & C_{12} & 0 & 0 & 0 \\ C_{12} & C_{11} & C_{12} & 0 & 0 & 0 \\ C_{12} & C_{12} & C_{11} & 0 & 0 & 0 \\ 0 & 0 & 0 & 4C_{44} & 0 & 0 \\ 0 & 0 & 0 & 0 & 4C_{44} & 0 \\ 0 & 0 & 0 & 0 & 0 & 4C_{44} \end{pmatrix}.$$

The strain in the system induces polarization $\mathbf{P}^{strain}$, which is proportional to the strain tensor

$$P_i^{strain}(\mathbf{r})=\sum_{k=1}^{6} e_{ik}(\mathbf{r})\varepsilon_k(\mathbf{r}) \tag{4}$$

In Eq. (4), $e_{ik}(\mathbf{r})$ is the piezoelectric tensor of GaN when $\mathbf{r}$ is inside the QD and the piezoelectric tensor of AlN when $\mathbf{r}$ is outside the QD. For WZ and ZB GaN/AlN QDs, the piezoelectric tensors are given as

$$e_{ik}^{WZ}=\begin{pmatrix} 0 & 0 & 0 & 0 & e_{15} & 0 \\ 0 & 0 & 0 & e_{15} & 0 & 0 \\ e_{31} & e_{31} & e_{33} & 0 & 0 & 0 \end{pmatrix};$$

$$e_{ik}^{ZB}=\begin{pmatrix} 0 & 0 & 0 & e_{14} & 0 & 0 \\ 0 & 0 & 0 & 0 & e_{14} & 0 \\ 0 & 0 & 0 & 0 & 0 & e_{14} \end{pmatrix}.$$

WZ GaN and WZ AlN exhibit spontaneous polarization $\mathbf{P}^{spont}$ with polarity specified by the terminating anion or cation at the surface. Since WZ GaN/AlN QDs are grown along the polar c-axis, only the z-component of the spontaneous polarization is nonzero:

$$P_i^{spont}(\mathbf{r})=P_{sp}(\mathbf{r})\,\delta_{iz}. \tag{5}$$

In Eq. (5), $P_{sp}(\mathbf{r})$ is the spontaneous polarization of WZ GaN when $\mathbf{r}$ is inside the QD and the spontaneous polarization of WZ AlN when $\mathbf{r}$ is outside the QD.

The total polarization,

$$\mathbf{P}(\mathbf{r})=\mathbf{P}^{strain}(\mathbf{r})+\mathbf{P}^{spont}(\mathbf{r}), \tag{6}$$

leads to the appearance of an electrostatic piezoelectric potential $V_p(\mathbf{r})$, which is found by solving the following Maxwell equation:

$$\nabla[\hat{\varepsilon}_{stat}(\mathbf{r})\nabla V_p(\mathbf{r})-4\pi\mathbf{P}(\mathbf{r})]=0. \tag{7}$$

In Eq. (7), $\hat{\varepsilon}_{stat}(\mathbf{r})$ is the dielectric tensor of GaN when $\mathbf{r}$ is inside the QD and the dielectric tensor of AlN when $\mathbf{r}$ is outside the QD. For WZ and ZB GaN/AlN QDs, the dielectric tensors are given as

$$\hat{\varepsilon}_{stat}^{WZ}=\begin{pmatrix} \varepsilon_{stat}^{\perp} & 0 & 0 \\ 0 & \varepsilon_{stat}^{\perp} & 0 \\ 0 & 0 & \varepsilon_{stat}^{\parallel} \end{pmatrix};$$

$$\hat{\varepsilon}_{stat}^{ZB}=\begin{pmatrix} \varepsilon_{stat} & 0 & 0 \\ 0 & \varepsilon_{stat} & 0 \\ 0 & 0 & \varepsilon_{stat} \end{pmatrix}.$$

All material parameters used in the calculation of the strain tensor and of the piezoelectric potential are listed in Table I.

Electron states are found as the eigenstates of the one-band envelope-function equation

$$\hat{H}_e\Psi_e=E_e\Psi_e, \tag{8}$$

where $\hat{H}_e$, Ψ_e, and E_e are the electron Hamiltonian, electron envelope wave function, and electron energy, respectively. The electron Hamiltonian $\hat{H}_e$ can be written as

$$\hat{H}_e=\hat{H}_S(\mathbf{r}_e)+H_e^{(\varepsilon)}(\mathbf{r}_e)+E_c(\mathbf{r}_e)+eV_p(\mathbf{r}_e), \tag{9}$$

where $\hat{H}_S$ and $H_e^{(\varepsilon)}$ are the kinetic and strain-dependent parts of the electron Hamiltonian, correspondingly, E_c is the energy of unstrained conduction band edge, e is the absolute value of electron charge, and V_p is the piezoelectric potential.

Hole states are found as the eigenstates of the six-band envelope-function equation

$$\hat{H}_h \Psi_h = E_h \Psi_h, \tag{10}$$

where $\hat{H}_h$ is the 6×6 matrix of the hole Hamiltonian, Ψ_h is the six-component column of the hole envelope wave function, and E_h is the hole energy. The hole Hamiltonian $\hat{H}_h$ can be written as

$$\hat{H}_h = \begin{pmatrix} \hat{H}_{XYZ}(\mathbf{r}_h) + H_h^{(\varepsilon)}(\mathbf{r}_h) & 0 \\ 0 & \hat{H}_{XYZ}(\mathbf{r}_h) + H_h^{(\varepsilon)}(\mathbf{r}_h) \end{pmatrix} + E_v(\mathbf{r}_h) + eV_p(\mathbf{r}_h) + H_{so}(\mathbf{r}_h), \tag{11}$$

where $\hat{H}_{XYZ}$ is a 3×3 matrix of the kinetic part of the hole Hamiltonian (including the crystal-field splitting energy for WZ QDs), $H_h^{(\varepsilon)}$ is a 3×3 matrix of the strain-dependent part of the hole Hamiltonian, E_v is the energy of the unstrained valence band edge, and H_{so} is the Hamiltonian of spin-orbit interaction.

It will be seen in the next section that the radius of the region of electron and hole localizations in the considered GaN/AlN QDs is less than the exciton Bohr radius of bulk GaN ($\sim$2 nm). Therefore, we can use the strong confinement approximation and calculate the exciton wave function as a product of electron and hole wave functions. Within this approximation, the exciton energy E_{exc} can be calculated considering the Coulomb potential energy $U(\mathbf{r}_e, \mathbf{r}_h)$ of the electron-hole system as a perturbation

$$E_{exc} = E_e - E_h + \int_V d\mathbf{r}_e \int_V d\mathbf{r}_h |\Psi_e(\mathbf{r}_e)|^2 |\Psi_h(\mathbf{r}_h)|^2 U(\mathbf{r}_e, \mathbf{r}_h), \tag{12}$$

where V is the total volume of the system.

The oscillator strength f of the transition corresponding to the exciton state with energy E_{exc} and envelope wave function $\Psi_e(\mathbf{r}_e)\Psi_h(\mathbf{r}_h)$ can be calculated as

$$f = \frac{E_P}{E_{exc}} \left| \int_V d\mathbf{r} \Psi_e(\mathbf{r}) \Psi_h^{(\alpha)}(\mathbf{r}) \right|^2, \tag{13}$$

where E_P is the Kane energy and α denotes the component of the hole wave function, which is active for a given polarization $\mathbf{e}$ of incoming light. The oscillator strength f defines the radiative lifetime τ written as

$$\tau = \frac{2\pi\varepsilon_0 m_0 c^3 \hbar^2}{n e^2 E_{exc}^2 f}, \tag{14}$$

where ε_0, m_0, c, and $\hbar$ are fundamental physical constants and n is the refractive index.

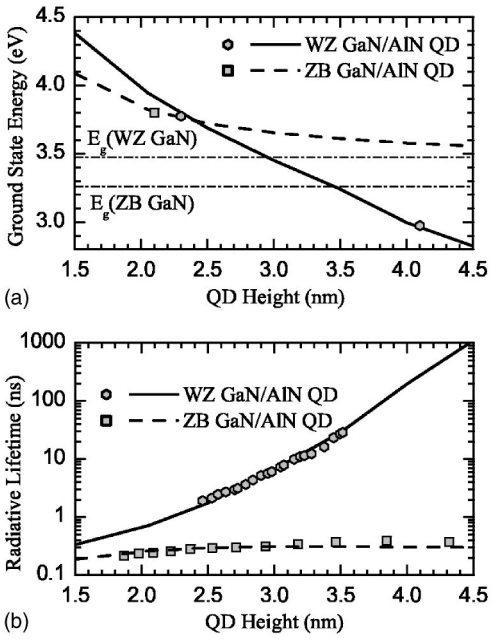

FIG. 1. Exciton ground state energy levels (a) and radiative lifetimes (b) as the function of QD height for wurtzite and zinc-blende GaN/AlN QDs. Dash-dotted lines in panel (a) indicate bulk energy gaps of wurtzite and zinc-blende GaN. Hexagons and squares represent experimental points from Refs. 3, 5, and 6 for wurtzite and zinc-blende QDs, respectively.

III. RESULTS AND DISCUSSION

Using the theory presented in the previous section one can calculate the optical spectra of WZ and ZB GaN/AlN QDs as a function of QD size. WZ (ZB) GaN/AlN QDs are modeled as a truncated hexagonal (square) pyramid on a wetting layer. The geometry of a WZ GaN/AlN QD with height H is described by the thickness of the wetting layer $w=0.5$ nm, QD bottom diameter $D_B=5(H-w)$, and QD top diameter $D_T=H-w$.[2,3] The corresponding dimensions for a ZB GaN/AlN QD with the same height can be described with $w=0.5$ nm, QD bottom base length $D_B=10(H-w)$, and QD top base length $D_T=8.6(H-w)$.[4,5] Material parameters used in our calculations have been taken from Ref. 7. The piezoelectric potential is neglected in the calculation of optical properties of ZB GaN/AlN QDs, because the maxima of the piezoelectric potential lie outside the ZB GaN/AlN QD and the magnitude of the piezoelectric potential is ten times less than it is in WZ GaN/AlN QDs.[7] In the following, we choose the coordinate system in such a way that the z-axis is directed along the growth direction, which is parallel to the c-axis for WZ QDs, and the x-axis is perpendicular to a QD edge lying on the wetting layer.

Figure 1(a) shows the results of our calculation of the exciton ground state energy levels while Fig. 1(b) shows the corresponding radiative lifetimes as a function of QD height for WZ and ZB GaN/AlN QDs. One can see from Fig. 1 that our calculations are in excellent agreement with the experimental data of Refs. 3, 5, and 6. As follows from the results for WZ GaN/AlN QDs higher than 3 nm, the exciton ground state energy drops below the bulk WZ GaN energy gap. Such a huge redshift of the exciton ground state energy with re-

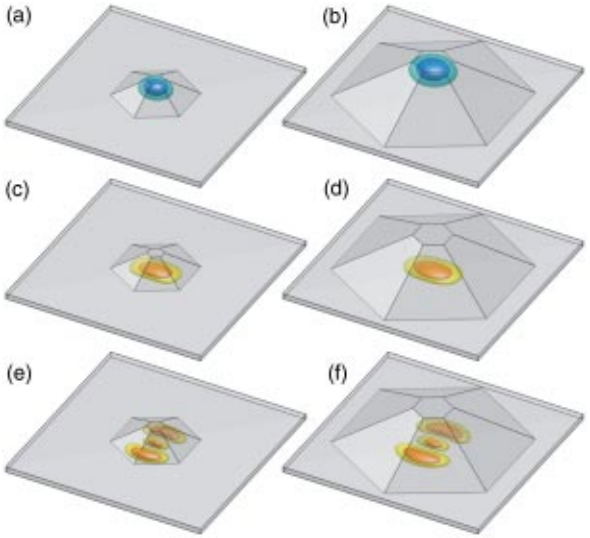

FIG. 2. Isosurfaces of probability density $|\Psi|^2$ for the electron ground state (a)–(b), the hole ground state (c)–(d), and an excited hole state (e)–(f) in wurtzite GaN/AlN QDs. Left-hand-side (a), (c), (e), and right-hand-side (b), (d), (f) panels correspond to QDs with height 2 and 4 nm, respectively. Dark (light) isosurfaces contain 1/3 (2/3) of the total probability density.

spect to the bulk WZ GaN energy gap is attributed to the strong piezoelectric field in WZ GaN/AlN QDs. Figure 1(b) shows that the radiative lifetime of the redshifted transitions in WZ GaN/AlN QDs ($H>3$ nm) is large and increases almost exponentially from 6.6 ns for QDs with height 3 nm to 1100 ns for QDs with height 4.5 nm. Analyzing Eqs. (13) and (14) one can conclude that the rapid increase of the radiative lifetime is caused by the rapid decrease of the electron-hole overlap with increasing QD height. The radiative lifetime in ZB GaN/AlN QDs is found to be on the order of 0.3 ns and almost independent of QD height.

The piezoelectric potential in a WZ GaN/AlN QD tilts conduction and valence band edges along the z-axis in such a way that it becomes energetically favorable for the electron to be located near the QD top and for the hole to be located in the wetting layer. Indeed, it is seen in Fig. 2 that the electron in WZ GaN/AlN QDs is pushed to the QD top, while the hole is localized in the wetting layer, near to the QD bottom. The deformation potential in both WZ and ZB GaN/AlN QDs bends the valence band edge in the xy-plane in such a way that it creates a paraboliclike potential well that tends to expel the hole from the QD side edges. Indeed, Figs. 2 and 3 show that the hole is expelled from the QD side edges.

Analyzing Figs. 2 and 3, one can notice two interesting effects. First, the increase of the QD size by a factor of two leads to a much smaller increase of the effective volume occupied by the electrons and holes. Second, for the depicted electron ground state and two first optically active hole states (for the incoming light polarized along the x-axis), the in-plane distribution of charge carriers in the ZB GaN/AlN QD resembles that in the WZ GaN/AlN QD if the coordinate system is rotated around the z-axis by $\pi/4$. Both phenomena can be explained by the effect of the strain field.

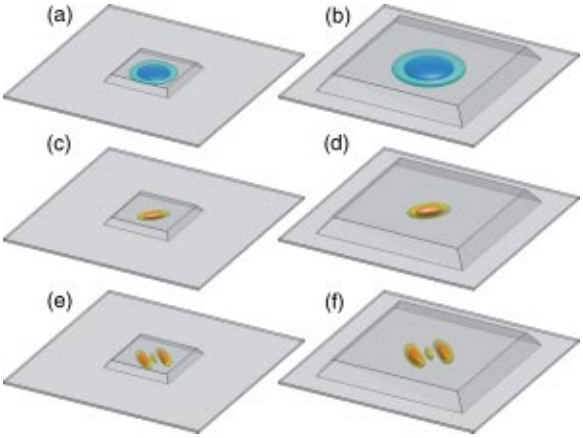

FIG. 3. The same as in Fig. 2, but for zinc-blende GaN/AlN QDs.

Figure 4 shows the results of the calculation of exciton energy levels and oscillator strengths corresponding to the first four optically active exciton states in WZ GaN/AlN QDs. The two states shown by solid (dashed) lines are active when the incoming light is polarized along the x-axis (y-axis). The exciton energy and oscillator strength in WZ GaN/AlN QDs depend on the in-plane polarization of the incoming light, because of the lack of the QD symmetry with the interchange of x and y coordinates. If the incoming light is randomly polarized in the x-y plane, each of the first two peaks in the absorption spectrum splits into a pair of two very close peaks. The distance between the two sets of peaks decreases from about 60 meV to about 40 meV with increasing the QD height from 1.5 to 4.5 nm. Such a relatively small decrease of the energy difference can be explained by the above-mentioned fact that the effective volume occupied by

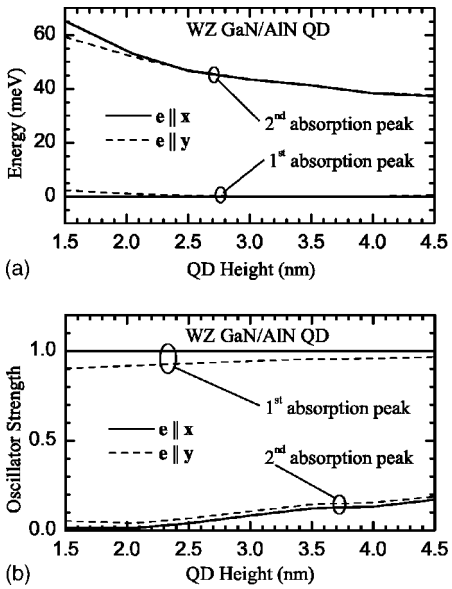

FIG. 4. Energy (a) and oscillator strength (b) of first four peaks in the absorption spectrum of wurtzite GaN/AlN QDs. Solid (dashed) lines correspond to the polarization of incoming light along the x-axis (y-axis). The energy in panel (a) and the oscillator strength in panel (b) are normalized to the first absorption peak when the light is polarized along the x-axis.

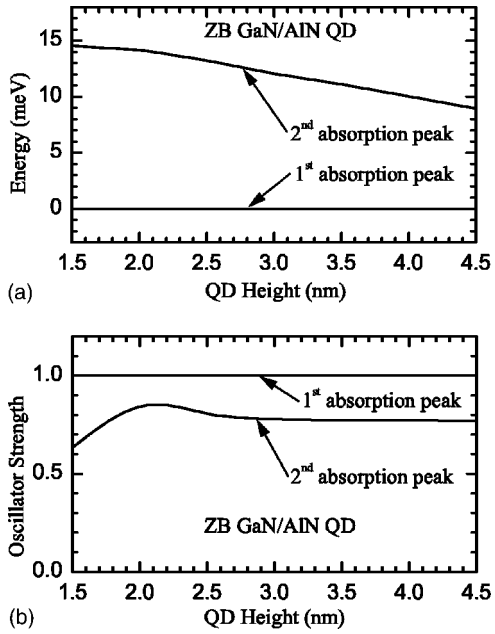

FIG. 5. Energy (a) and oscillator strength (b) of first two peaks in the absorption spectrum of zinc-blende GaN/AlN QDs. The energy in panel (a) and the oscillator strength in panel (b) are normalized to the first absorption peak.

electrons and holes increases only slightly with increasing the QD size. Figure 4(b) shows that the amplitude of the second set of absorption peaks is about ten times smaller than it is for the first set of absorption peaks and it slightly increases with increasing the QD size.

Figure 5 shows the calculated exciton energy levels and oscillator strengths corresponding to the first two optically active exciton states in ZB GaN/AlN QDs. Each of the two states shown in Fig. 5 is two-fold degenerate due to the QD symmetry with the interchange of x and y coordinates. The distance between the first two peaks in the absorption spectrum decreases from about 15 meV to about 10 meV with increasing the QD height from 1.5 to 4.5 nm. Similarly to WZ GaN/AlN QDs, such a relatively small decrease of the energy difference can be explained by the fact that the effective volume occupied by electrons and holes increases only slightly with increasing the QD size. However, because the lateral size of ZB QDs is about two times the lateral size of WZ QDs, the energy difference between the first two absorption peaks in ZB QDs is about four times smaller than it is in the WZ QDs. Figure 5(b) shows that unlike WZ GaN/AlN QDs, the amplitude of the second absorption peak in ZB GaN/AlN QDs is comparable with the amplitude of the first absorption peak and it changes non-monotonically with increasing QD size.

IV. CONCLUSIONS

We have carried out the theoretical calculation and comparison of optical properties of WZ and ZB GaN/AlN QDs with heights from 1.5 to 4.5 nm. It has been established that the built-in piezoelectric field at the GaN/AlN interface governs optical properties of WZ QDs while having a small effect on ZB QDs. The major difference in optical response of the two types of QDs is that the radiative lifetime in WZ GaN/AlN QDs increases exponentially with QD height, whereas it is almost constant in ZB GaN/AlN QDs. Calculated properties of the exciton ground states in both types of QDs are in good agreement with available experimental data for all considered QD sizes. The ratio of the second peak to the first peak in the absorption spectrum is close to 0.1 for WZ QDs and close to 1 for ZB QDs. Reported theoretical results for the optical spectra of GaN/AlN QDs can be used for interpretation of experimental data and optimization of the QD structures for optoelectronic applications.

ACKNOWLEDGMENTS

This work was supported in part by the NSF-NATO 2003 award to V.A.F. and by the DMEA/DARPA CNID Program No. A01809-23103-44 and U.S. CRDF Award No. MP2-3044 to A.A.B. The authors acknowledge useful discussions with Professor E.P. Pokatilov (MSU).

[1]B. Daudin, F. Widmann, G. Feuillet, Y. Samson, M. Arlery, and J. L. Rouviere, Phys. Rev. B **56**, R7069 (1997).
[2]F. Widmann, B. Daudin, G. Feuillet, Y. Samson, J. L. Rouviere, and N. Pelekanos, J. Appl. Phys. **83**, 7618 (1998).
[3]F. Widmann, J. Simon, B. Daudin, G. Feuillet, J. L. Rouviere, N. T. Pelekanos, and G. Fishman, Phys. Rev. B **58**, R15989 (1998).
[4]E. Martinez-Guerrero, C. Adelmann, F. Chabuel, J. Simon, N. T. Pelekanos, G. Mula, B. Daudin, G. Feuillet, and H. Mariette, Appl. Phys. Lett. **77**, 809 (2000).
[5]B. Daudin, G. Feuillet, H. Mariette, G. Mula, N. Pelekanos, E. Molva, J. L. Rouviere, C. Adelmann, E. Martinez-Guerrero, J. Barjon, F. Chabuel, B. Bataillou, and J. Simon, Jpn. J. Appl. Phys., Part 1 **40**, 1892 (2001).
[6]J. Simon, N. T. Pelekanos, C. Adelmann, E. Martinez-Guerrero, R. Andre, B. Daudin, L. S. Dang, and H. Mariette, Phys. Rev. B **68**, 035312 (2003).
[7]V. A. Fonoberov and A. A. Balandin, J. Appl. Phys. **94**, 7178 (2003).
[8]V. A. Fonoberov, E. P. Pokatilov, and A. A. Balandin, J. Nanosci. Nanotechnol. **3**, 253 (2003).